ACCOUNTS
of chemical research

Tailor-Made Rylene Arrays for High Performance n-Channel Semiconductors

Wei Jiang, Yan Li, and Zhaohui Wang*

Beijing National Laboratory for Molecular Sciences, Key Laboratory of Organic Solids, Institute of Chemistry, Chinese Academy of Sciences, Beijing 100190, P. R. China

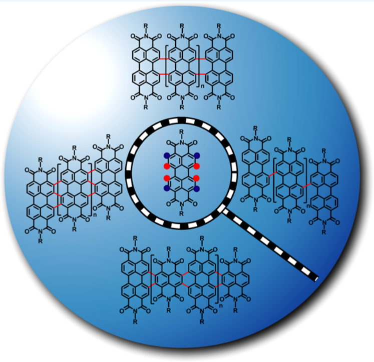

CONSPECTUS: Rylene dyes, made up of naphthalene units linked in *peri*-positions, are emerging as promising key building blocks to create π-functional materials. Chemists have found uses for these ribbonlike structures in a wide range of applications of optoelectronic devices. Because their structure combines two sets of six-membered electron-withdrawing dicarboxylic imide rings, rylene diimides exhibit enhanced solubility, excellent chemical and thermal stabilities, high electron affinities, and remarkable electron-transporting properties. Among them, perylene diimide (PDI) and naphthalene diimide (NDI) derivatives are important representatives improving the performance of electron-transporting technologies, relative to their p-channel counterparts.

Pioneering works by Müllen and Langhals have inspired chemists to extend the π-conjugation along the *peri*-positions of rylene diimides, which generally results in impressive bathochromic shifts and a nearly linear increase in the extinction coefficient. In addition, in the past years, researchers have focused on π-expansion of NDI or PDI systems through *bay*-functionalization with carbocyclic and heterocyclic rings annulated onto the skeleton. However, chemists have rarely investigated lateral expansion via both *bay*- and *nonbay*-functionalization to construct homologous series of rylene arrays with different electronic delocalization and fine-tuned flexible linkage. This is probably due to the lack of effective procedures for the (multi) carbon−carbon formation and annulation of electron-deficient rylene imide units.

In this Account, we discuss our recent progress in the design and synthesis of laterally expanded rylene dyes based on homocoupling and cross-coupling reactions of core-functionalized PDIs and NDIs to achieve novel high performance n-channel organic semiconducting materials. These new achievements offer us opportunities to learn fundamental issues about how chemical and physical properties alter with incremental changes in structure. We highlight synthetic methodology of transition-metal mediated coupling reactions (and/or C−H transformation) for singly linked, doubly linked, and fully conjugated triply linked oligoPDIs, and further for the construction of hybrid rylene arrays via *bay*- and/or *nonbay*-functionalization. In addition, we summarize the informative correlations between the molecular structures and their optoelectronic properties, especially the modulation of progressively red-shifted absorption maxima and positive shifts in the redox potentials. This decreases the energy gaps and increases the electron-accepting abilities through expansion of π-system, which has direct impacts on the compounds' potential applications in optoelectronic devices. Finally, we introduce the promising applications of these laterally expanded rylene dyes as exceptional high performance n-channel semiconductors in organic field-effect transistors (OFETs) and competitive candidates for non-fullerene acceptors in high efficient organic photovoltaic devices (OPVs).

1. INTRODUCTION

Organic semiconducting materials (OSCs) are key components in next-generation optoelectronic devices.[1] Their unique features as structural versatility can be efficiently tuned by chemical synthesis and functionalization to afford an exciting library of π-conjugated systems that meet the required criteria for diverse applications.[2−5] For instance, organic field-effect transistors (OFETs) and photovoltaic devices (OPVs) have been spurring increasing attention based on p- (hole-transporting) and/or n-channel (electron-transporting) OSCs.[6,7] More encouragingly, significant advancement on both diversity and high-performance for p-channel semiconductors has been achieved to offer present hole mobilities comparable to traditional silicon in OFETs and power conversion efficiencies (PCEs) exceeding 10% in OPVs.[8,9]

Nevertheless, n-channel counterparts with high mobility, good processability and air-stability fulfilling for applicable optoelectronics are still highly desirable, since they are essential blocks for construction of organic p−n junction and complementary logic circuits, also for developing highly efficient electron-transporting transistors and OPVs.[10] The ideal high-performance n-channel OSCs should exhibit the following set of properties: (i) effective packing arrangement for favorable electron transporting; (ii) appropriate electron affinity to facilitate electron injection in OFETs or exciton separation in OPVs; (iii) ambient stability with LUMO energy levels for antioxidation in air; (iv) good processability for the requirement of balancing of molecular packing and solubility in

Received: June 29, 2014
Published: September 29, 2014

dx.doi.org/10.1021/ar500240e | *Acc. Chem. Res.* 2014, 47, 3135−3147

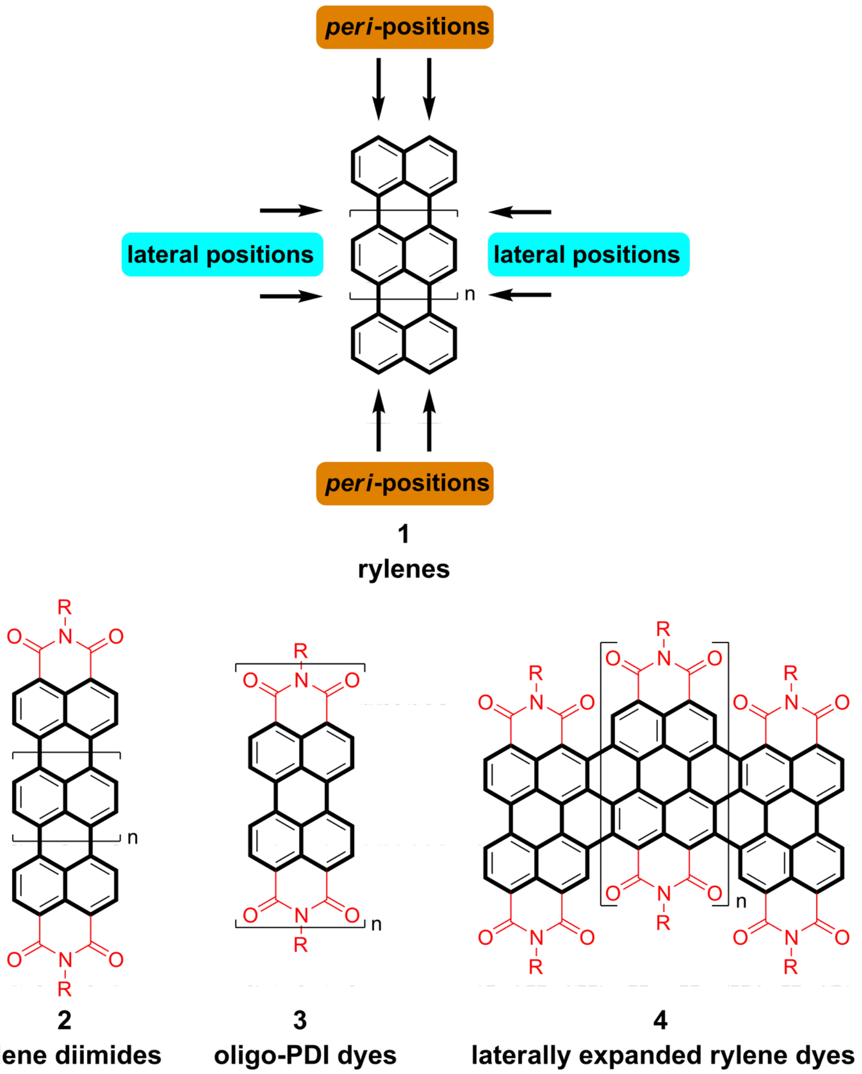

1
rylenes

2
rylene diimides

3
oligo-PDI dyes

4
laterally expanded rylene dyes

Figure 1. Chemical structures of rylenes (**1**), rylene diimides (**2**), oligo-PDI dyes (**3**), and laterally expanded rylene dyes (**4**).

rigid π-conjugated systems. Although detailed studies by many groups in the past years have brought steady progress in this field, there still has been scarcity of such molecules synergistically integrated with synthetic availability to maximize their performances.

Rylene dyes, made up of naphthalene units linked in *peri*-positions, have attracted intensive attention in both theoretical and synthetic chemistry due to their perfect graphene-ribbon-like structures and attractive properties, since first reported by E. Clar in 1948 (**1**, Figure 1).[11] Two kinds of functionalization positions are termed as *peri*-positions and lateral positions including *bay*- and *nonbay*-regions, respectively. Particularly, imide-functionalization endows rylene diimides enhanced solubility, chemical and thermal stabilities, and, more importantly, excellent electron-transporting characteristics.[12] Recent interest in these dyes focused on chemical modifications both on the skeleton and at imide-positions. Perylene diimides (PDIs) and naphthalene diimides (NDIs) are considered as the most promising building blocks in the rylene family to close the gap in electron-transporting performance in comparison to that of their p-channel counterparts.[13] The past decade witnessed an effective core-enlargement of NDI or PDI system either at *peri*-functionalization (π-extension along the long molecular axis) or at *bay*-functionalization (π-expansion along the short molecular axis), which offered a variety of desirable properties and flexible tunability.[14,15] In addition, Müllen et al. inspired a synthetic approach to obtain homologous series of rylene diimides from perylene to hexarylene diimides (**2**), which realized progressively red-shifted absorption to the NIR region,[16] while the "intense" dyes based on oligo-PDI dyes with remarkably high absorptivity have been pioneered by Langhals and Jona (**3**).[17] Despite all the progress in the chemical modification of rylene dyes, developing an efficiently synthetic method for lateral expansion via both *bay*- and *nonbay*-functionalization to construct homologous series of rylene arrays still remains a great challenge in organic and materials chemistry.

This Account highlights our recent progress in the design and synthesis of laterally expanded rylene dyes based on homocoupling and cross-coupling reactions of core-functionalized PDIs and NDIs as well as their potential optoelectronic applications. Our findings suggest that rylene dyes could be harnessed to achieve effective lateral expansion by connecting identical or two types of chromophores through rational designing strategies. These new avenues for the fascinating chemistry of highly π-expanded rylenes enrich the library of electron-deficient molecular systems aiming at generating high-performance n-channel OSCs with good ambient stability and processability.

2. SYNTHESIS OF LATERALLY EXPANDED RYLENE ARRAYS

Homologous series of rylene arrays with a fine-tuned linked nature are particularly exciting and interesting because they could offer fundamental information about how chemical and physical properties alter with incremental changes in structure. Two synthetic strategies were proved to be successful for the chemical modification and functionalization of rylenes. Swallow-tail type solublizing substitutents were first imparted at imide-positions by Langhals,[18] while Seybold and Wagenblast at BASF first mastered the *bay*-region chemistry based on halogenated PDIs through nucleophilic substitution.[19] Although the successful introduction of halogen atoms also motivated many endeavors to chemical transformations by exercising various transition-metal catalyzed coupling reactions, the homologous series of rylenes arrays remained largely an unsolved issue. The fundamental obstacle to solving this conundrum is the lack of a simple synthetic transformation avoiding dehalogenation. We start our journey of laterally expanded rylene arrays bearing different *bay*-linkages by copper-mediated Ullmann-type homocoupling reactions.

2.1. Singly Linked OligoPDIs

Monobromo- and dibromo-substituted PDIs,[20] which are key intermediates for the synthesis of *bay*-region functionalized derivatives, are suitable building blocks for the construction of singly linked rylene arrays. The classical Ullmann coupling reactions are copper-catalyzed reactions for aryl—aryl bond formation,[21] and recent development has been achieved on the modification of this type of reactions which are mostly attributed to the utilization of some special ligands.[22] We found with a big surprise that when 1-BrPDIs (**5**) was stirred in dry dimethyl sulfoxide (DMSO) with a stoichiometric amount of nanosized copper powder, thus s-diPDIs (**6**) could be obtained in high yield.[23,24] While 1,7-2BrPDI (**7**) was chosen as the starting material, well-defined singly linked oligoPDIs, from dimer (**6a**), trimer (**8**), and higher oligomers (**9**) up to octadecamer, could be achieved following the similar conditions (Scheme 1).[23] It should be noted that when the reaction temperature was lowered to 30 °C, s-2BroligoPDIs (**10**) with reserved two bromine atoms could be found, which is very important for subsequent C—C bond formation and lateral position modification. We attributed this extremely straightforward successful homocoupling of brominated PDIs to the activated effect of two strong electron-withdrawing imide groups and better reactivity of nanosized copper powder.

2.2. Doubly Linked OligoPDIs

It would be certainly interesting to realize doubly linked PDI arrays, in which the PDI units were directly bonded via two C—C bonds, rather than in singly linked mode. For this purpose, we envisaged that tetrahalogen-substituted PDIs, such as 1,6,7,12-4ClPDIs and 1,6,7,12-4BrPDIs, are served as perfect building blocks. Accordingly, the homocoupling of **13** proceeded smoothly through copper-mediated Ullmann coupling (or with Pd(PPh$_3$)$_4$ as the additive) to afford the desired d-4CldiPDIs **14** bearing both aryl and aliphatic chains.[25,26] The higher oligomers (**15** and **16**) up to tetradecamer could be detected by MALDI-TOF with reserving four chlorine atoms at *bay*-regions for further functionalization (Scheme 2).[25] Because of the tetraphenylene architecture between PDI subunits, this kind of oligomer possessed highly twisted and locked ladder-type structures with perpendicularly entangled PDI moieties, and thus expressed good solution processabilities in common organic solvents. We also examined the homocoupling of 1,12-dihalogenated PDIs (1,12-2XPDIs, **11**)[27] with two halogen atoms in the same *bay*-region to afford halogen-free dimers (**12**).[23,24] Remarkably, the dimer (**14a**) and trimer (**15**) were able to isolate pure enantiomers that demonstrated stable chirality owing to the racemization barriers, which was further proved by CD spectra being in agreement with computed ones.[25] The first successful construction of chiral ladder-type PDIs arrays with extremely twisted structures in PDI family is truly remarkable, which renders promising candidates for applications in special optoelectronic devices, enantioselective recognition, and chiral supramolecules.

Scheme 1. One-Pot Synthesis of Singly Linked OligoPDIs

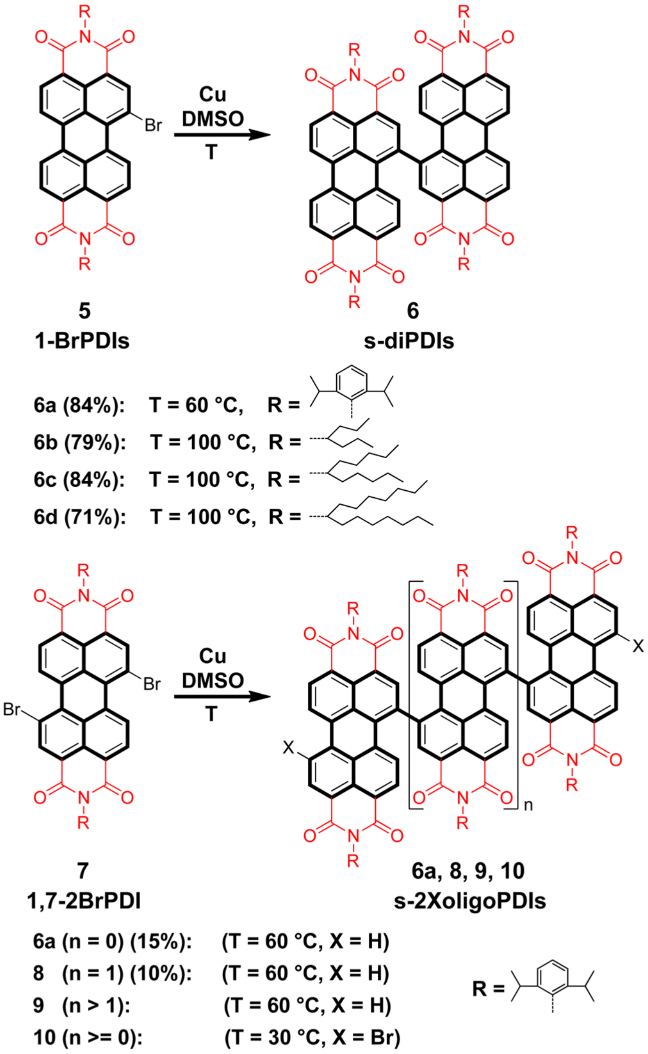

2.3. Triply Linked OligoPDIs

The successful development of singly and doubly linked oligoPDIs provides an initial model for construction of laterally expanded oligoPDIs by direct Ullmann C—C bonding via *bay*-region functionalization. Whereas triply linked oligoPDIs have a larger fully conjugated structure and more rigid skeleton, which require more reactive positions and effective synthetic method for multiple C—C bond formation involving *nonbay*-regions. We initially used stoichiometric amount of CuI, L-proline, and K$_2$CO$_3$ as the reagents, to trigger the Ullmann homocoupling of

Scheme 2. One-Pot Synthesis of Doubly Linked OligoPDIs

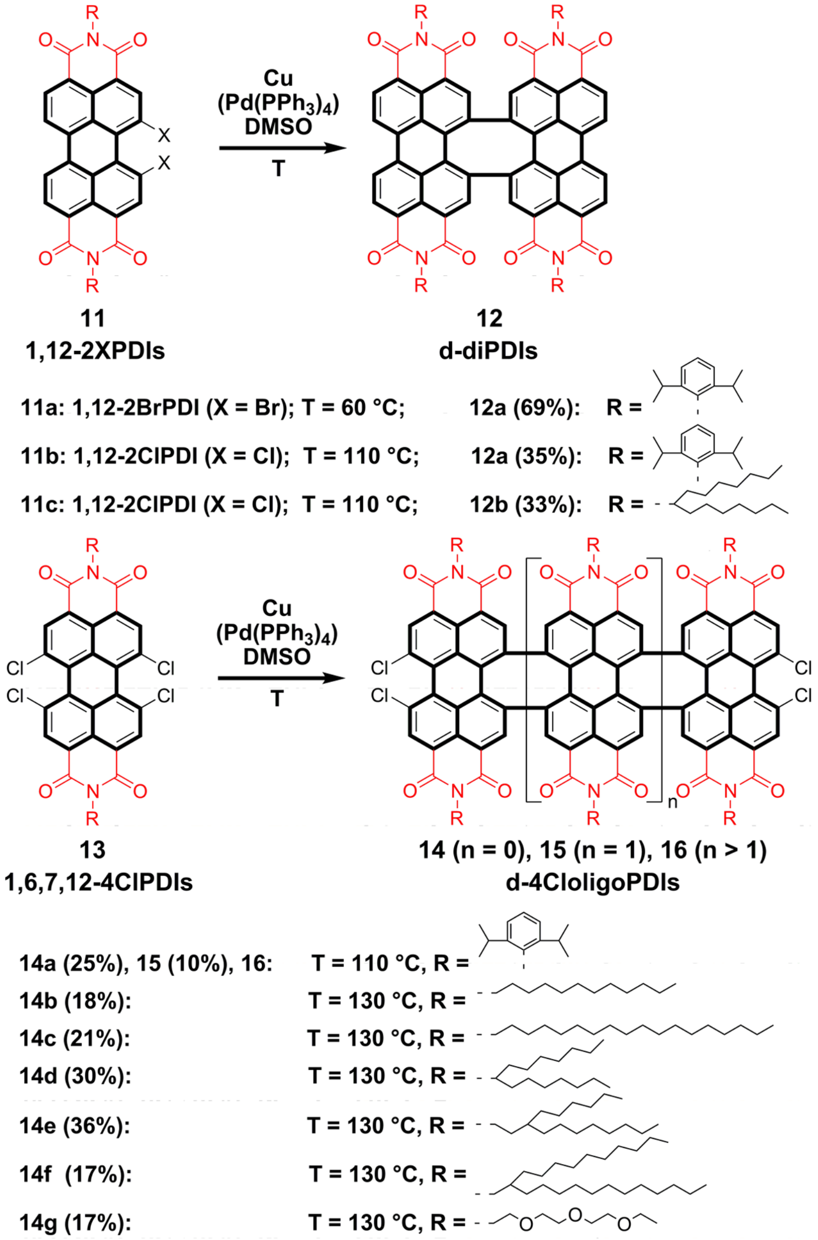

13a. Fully conjugated triply linked diPDI (**18a**) without any halogen atoms was successfully synthesized in moderate yield at 110 °C via the combination of Ullmann coupling and C−H transformation, which represents the first step toward the laterally expanded oligoPDIs via both *bay*-region and *nonbay*-region functionalization (Scheme 3).[28]

Importantly, we further found that the reaction temperature has a pivotal influence on the retaining of chlorine atoms. For example, t-4CldiPDI (**20a**) was produced under the same catalytic conditions at decreased temperature of 75 °C.[28] In addition, more halogenated derivatives (t-4BrdiPDI, **22** and t-4IdiPDI, **23**) could also be obtained at relatively lower reaction temperature.[29] It should be noted that in the synthesis of t-4XdiPDIs, *monobay*-dihalogenated diPDIs (**19** or **21**) could be also prepared as byproducts.[27] Starting from *monobay*-dihalogenated PDIs (**11**), t-diPDIs (**18**) was generated following the same conditions,[23] which provided an important clue to the comprehension of copper-mediated coupling mechanism. A plausible mechanism have been proposed that the *monobay*-copper-chelated PDI complex acting as a key intermediate initiates the synergetic reactions to afford either tetrahalogenated t-diPDIs under basic conditions or *monobay*-dihalogenated t-diPDIs when quenched with aqueous acid.[27] We also demonstrated a cost-effective protocol avoiding ligand to afford t-4CldiPDIs using $CuCl_2$ as the catalyst, *t*BuOK as the base, and $n\mathrm{Bu}_4\mathrm{NI}$ as the additive.[30]

The synthetic chemistry of t-diPDIs and the retaining halogen atoms on the edges provide a feasible way to both the next chemical modification at their *bay*-regions and the construction of higher oligomers. Thus, a new family of highly twisted systems (**24**) by doubly bonding linkage was obtained via the combination of the structural features of almost planar triply linked diPDI and deformationally doubly linked diPDI unit.[26] We followed our synthetic strategies toward S-PDI[31] to develop 2S-diPDI and 2NPh-diPDI (**25a** and **25c**) either by Stille coupling or Buchwald-Hartwig reaction, respectively.[32]

Scheme 3. One-Pot Synthesis of Triply Linked DiPDIs

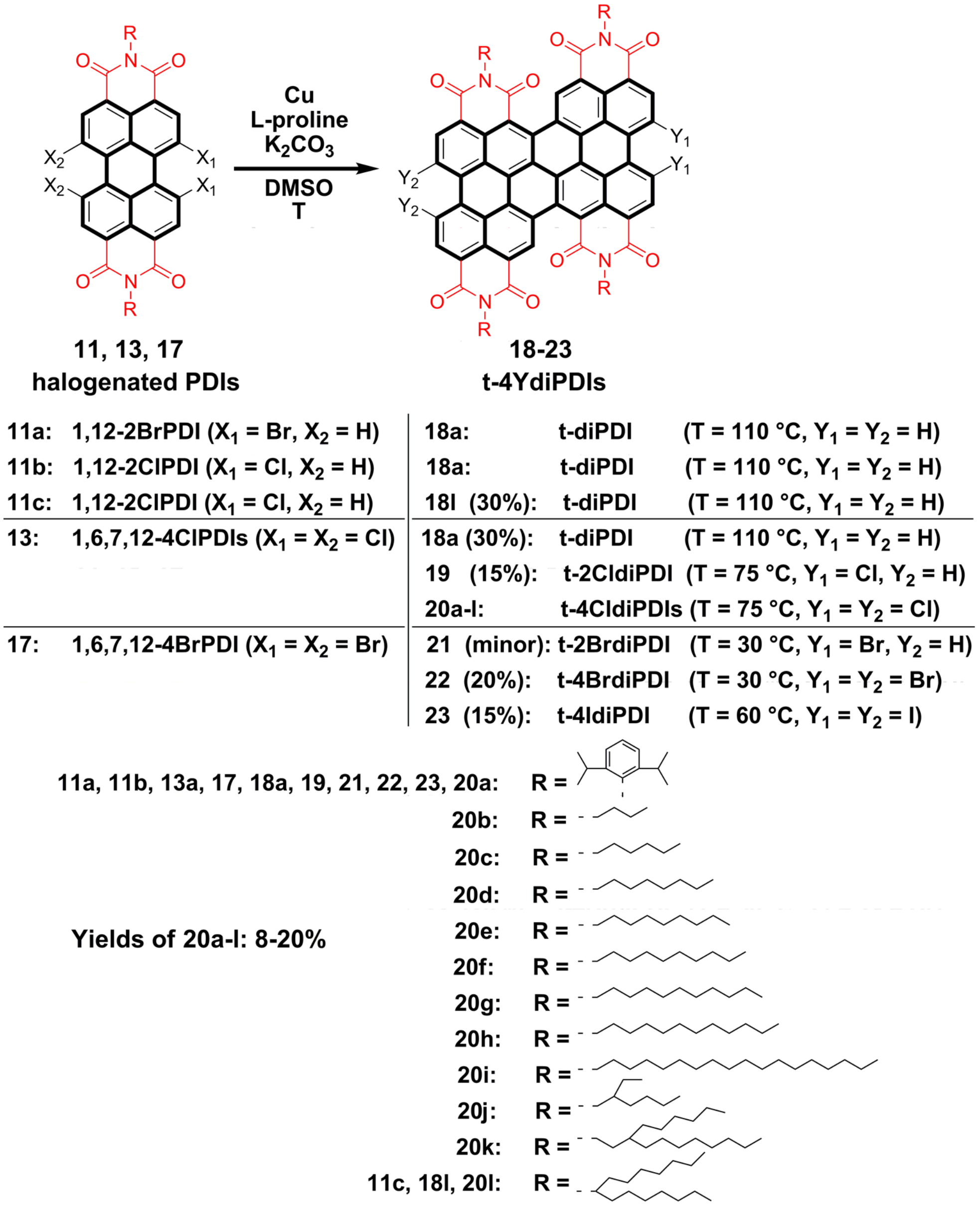

11a: 1,12-2BrPDI (X_1 = Br, X_2 = H)	18a:	t-diPDI	(T = 110 °C, Y_1 = Y_2 = H)
11b: 1,12-2ClPDI (X_1 = Cl, X_2 = H)	18a:	t-diPDI	(T = 110 °C, Y_1 = Y_2 = H)
11c: 1,12-2ClPDI (X_1 = Cl, X_2 = H)	18l (30%):	t-diPDI	(T = 110 °C, Y_1 = Y_2 = H)
13: 1,6,7,12-4ClPDIs (X_1 = X_2 = Cl)	18a (30%):	t-diPDI	(T = 110 °C, Y_1 = Y_2 = H)
	19 (15%):	t-2CldiPDI	(T = 75 °C, Y_1 = Cl, Y_2 = H)
	20a-l:	t-4CldiPDIs	(T = 75 °C, Y_1 = Y_2 = Cl)
17: 1,6,7,12-4BrPDI (X_1 = X_2 = Br)	21 (minor):	t-2BrdiPDI	(T = 30 °C, Y_1 = Br, Y_2 = H)
	22 (20%):	t-4BrdiPDI	(T = 30 °C, Y_1 = Y_2 = Br)
	23 (15%):	t-4IdiPDI	(T = 60 °C, Y_1 = Y_2 = I)

Yields of 20a-l: 8-20%

Compared with extremely distorted structures of tetrahalogenated diPDIs, the introduction of steric congestion in *nonbay*-regions and the concurrent formation of five-membered heterocycles strain in *bay*-regions confirmed their extraordinary doubly bowl-shaped structures by single-crystal structure analysis. Another chalcogen-incorporated derivative, 2Se-diPDI (**25b**) was synthesized by reacting t-4CldiPDI (**20a**) and Na_2Se in *N,N*-dimethylformamide (DMF), and a series of *monobay*-functionalized N-diPDIs featuring ethyl benzoate (PhCOOEt) (**26a**), triphenylamine (TPA) (**26b**), and Pd-tetraphenylporphrin (PdTPP) (**26c**), and diPDI-N(Flu)N-diPDI (**27**) sandwiching a fluorene unit were prepared by cross-coupling of t-2CldiPDI (**19**) with corresponding amines under Buchwald-Hartwig coupling conditions (Figure 2).[27,33,34]

Apart from dimers, t-triPDIs (**28a**, **29a**) and/or other higher oligoPDIs as the minor products as dark-green solids could be observed in the mixtures in the course of homocoupling of 1,6,7,12-4ClPDIs. Likewise, 1,6,7,12-4BrPDI with four more active bromine atoms easily further underwent the coupling reaction at 110 °C and produced halogen-free t-triPDIs (**28b**, **29b**).[35] Accordingly, we utilized t-4CldiPDI (**20a**) instead of 1,6,7,12-4ClPDI (**13a**) as the precursor and conducted the coupling reaction at 110 °C under the catalytic system of Cu/$Pd(PPh_3)_4$; thus, t-4CltetraPDIs (**30**) could be obtained in close to 10% yields.[36] Theoretically, there should be two isomeric structures for trimers (Scheme 4), and three isomeric structures for tetramers (Scheme 5) due to the two possible coupling sites. In fact, only two of them (**30a** and **30b**) were achieved primarily in this reaction for tetramers, probably due to better stability for more symmetrical structures. It was necessary to purify these isomers by cyclic high performance liquid chromatography (HPLC) due to their big π-conjugated structures and similar polarity.

2.4. Hybrid Rylene Dyes

To avoid multiple isomeric structures of higher homologous series, we designed and constructed hybrid rylene arrays by lateral fusion of PDI or t-diPDI and NDI units via Stille-type cross-coupling and C−H transformation (Scheme 6). NDI tin

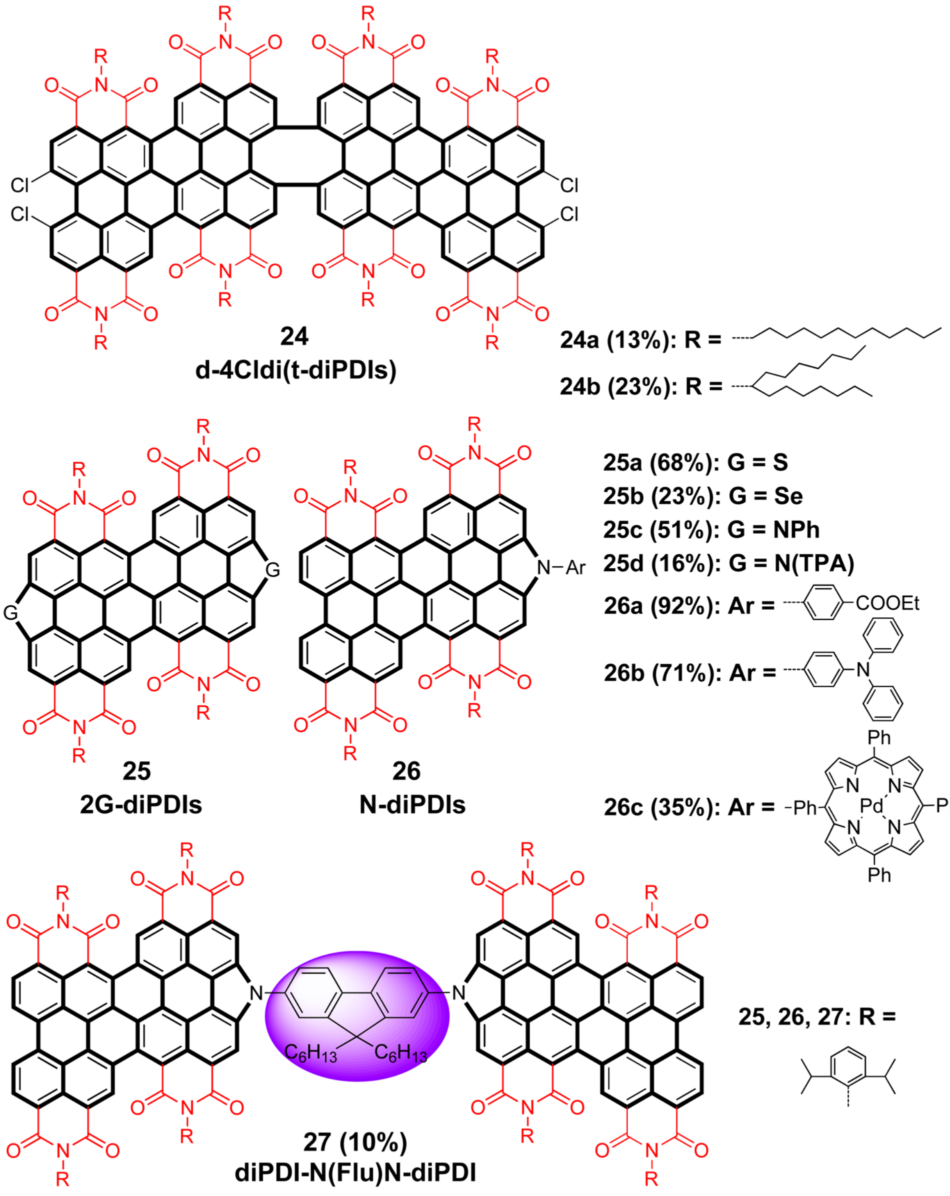

Figure 2. Functionalized derivatives based on t-diPDIs.

derivatives have been recently examined by the corresponding brominated NDIs reacting with Bu_3Sn-$SnBu_3$ in $Pd_2(dba)_3$/$P(o\text{-tol})_3$/toluene systems, suggesting important building blocks for construction of hybrid rylene dyes.[37]

Monobay-dichlorinated diPDI (**11b**) were initially chosen as model substrates to react with 2-stannyl NDI (**31**) in the presence of $Pd(PPh_3)_4$ and CuI as an additive. Fused hybrid NDI-PDI (**32**) was successfully afforded accompanied by singly linked byproduct (**33**).[38] Encouraged by the success of this annulation, readily available 1,6,7,12−4ClPDIs (**13**) were used to check the scope of this method and find that a series of fully conjugated NDI-PDI-NDI derivatives (**34**) could be obtained in higher yields using only $Pd(PPh_3)_4$ as the catalyst.[38] This method has been employed to produce series of NDI-diPDI-NDI (**35**) that further enriched the library of the π-expanded rylenes.[39] Different substituents in imide positions of NDIs and PDIs could be incorporated to tune self-assembly properties of these hybrid dyes.

3. ELECTRICAL AND OPTICAL PROPERTIES OF LATERALLY EXPANDED RYLENE ARRAYS

The design, synthesis, and characterization of laterally expanded rylene arrays inspire the new development of promising candidates in optoelectronic devices. Structurally, theses molecular systems consist of well-recognized high performance electron-transporting units, imbuing them with unique electrical and optical properties that can be easily tuned via rational and straightforward chemical modifications. The expansion of π-system will induce a significant charge delocalization, thus the resulting molecules will undergo a bathochromic shift in the absorption maximum and a positive shift in the redox potentials, indicating the decrease in the energy gaps and the increase in electron-accepting abilities.

3.1. *Bay*-Linked Rylene Dimers

We first select four *bay*-linked rylene dimers (compounds **6a**, **12a**, **18a**, and **32**) for systematically investigation of their optical, electrochemical, and equilibrium structures (Table 1). Among them, singly and doubly linked dimers (**6a** and **12a**)

Scheme 4. One-Pot Synthesis of Triply Linked TriPDIs

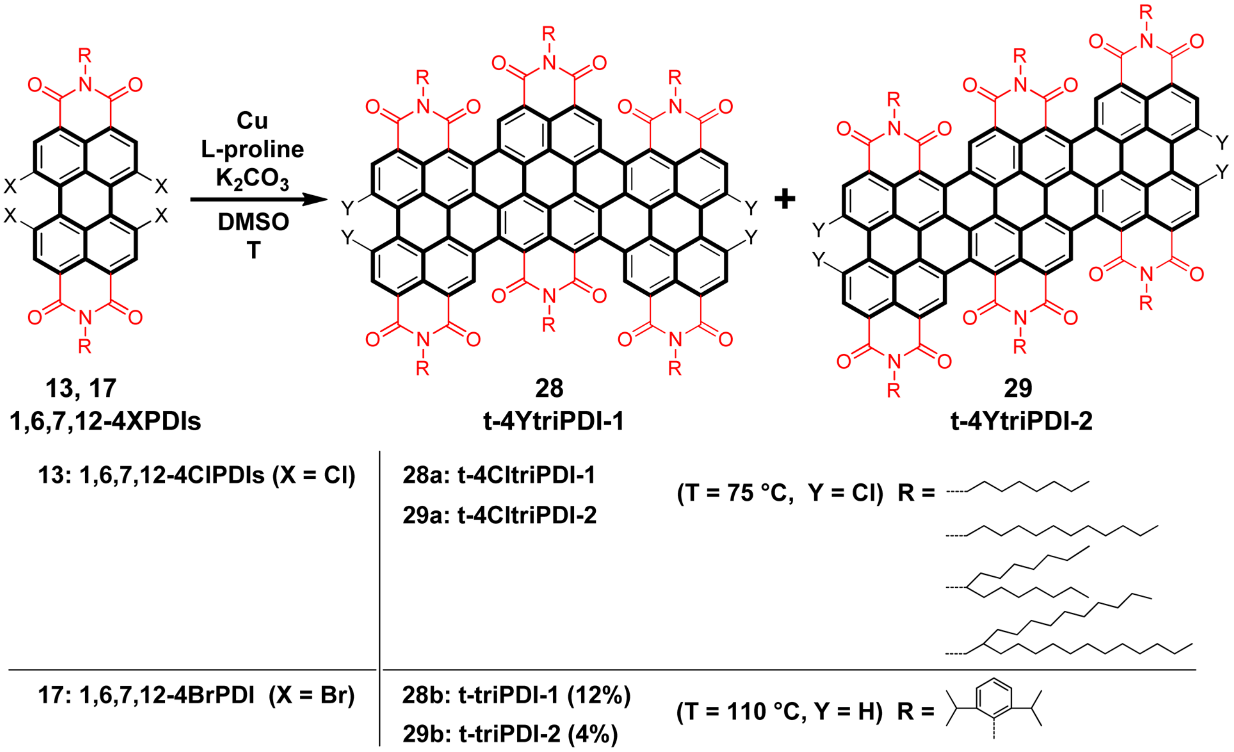

13, 17
1,6,7,12-4XPDIs

28
t-4YtriPDI-1

29
t-4YtriPDI-2

13: 1,6,7,12-4ClPDIs (X = Cl)

28a: t-4CltriPDI-1
29a: t-4CltriPDI-2

(T = 75 °C, Y = Cl) R =

17: 1,6,7,12-4BrPDI (X = Br)

28b: t-triPDI-1 (12%)
29b: t-triPDI-2 (4%)

(T = 110 °C, Y = H) R =

Scheme 5. One-Pot Synthesis of Triply Linked TetraPDIs

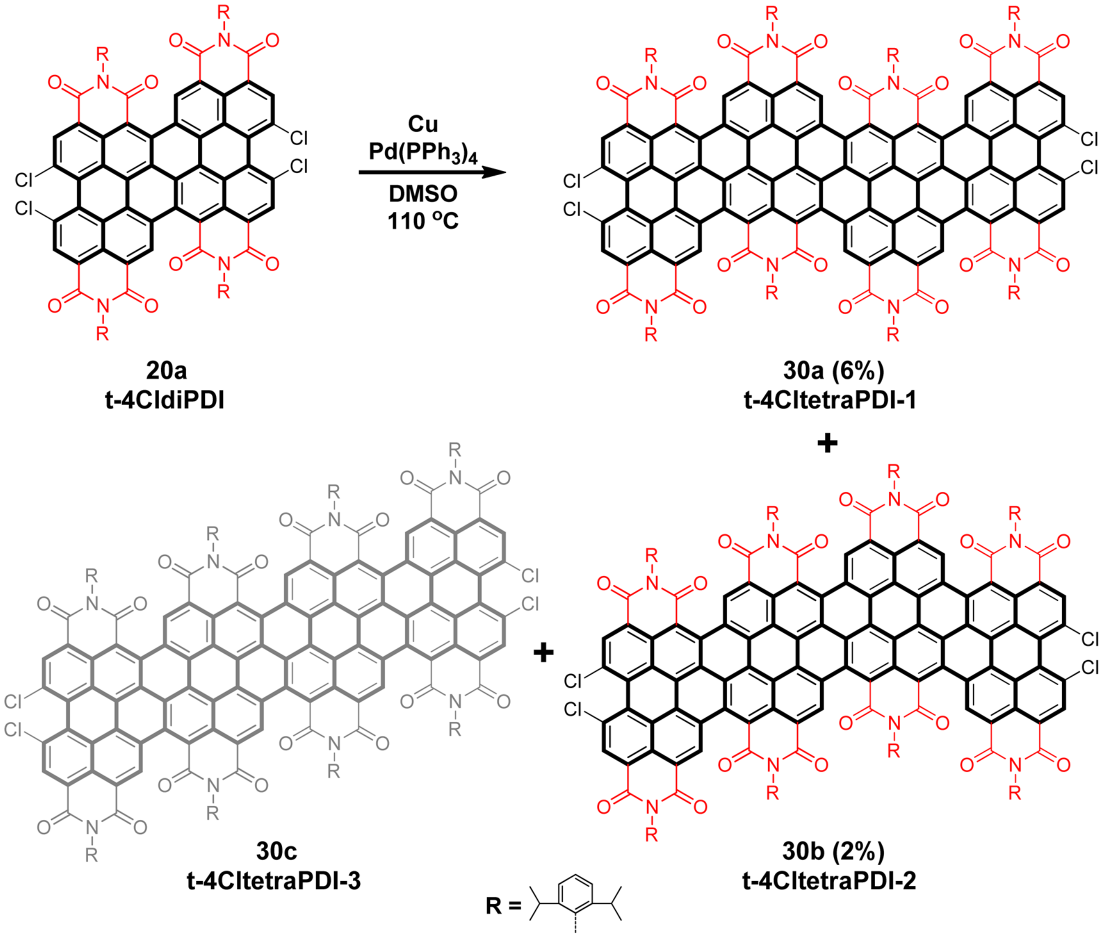

20a
t-4CldiPDI

30a (6%)
t-4CltetraPDI-1

30c
t-4CltetraPDI-3

30b (2%)
t-4CltetraPDI-2

Scheme 6. One-Pot Synthesis of Hybrid Rylene Dyes

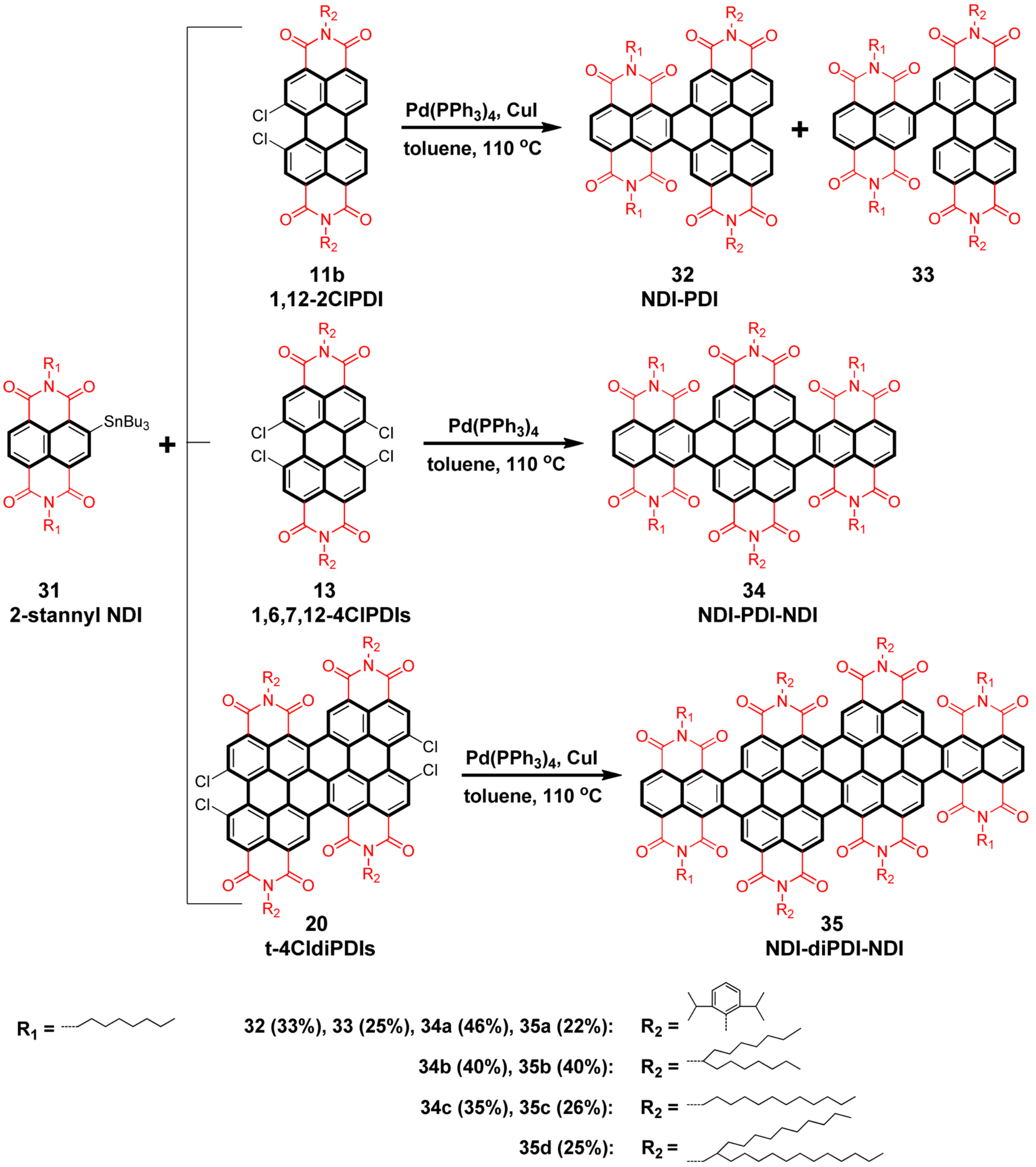

Table 1. Photophysical Properties of Rylene Dimers

compds	λ_{abs} (nm)	ε (M^{-1} cm^{-1})	E_{1r} (V)	E_{2r} (V)	E_{3r} (V)	E_{4r} (V)	E_{LUMO} (eV)[c]	E_g (eV)	ref
NDI[a]	380	54 243	−1.03	−1.51			−3.90	3.12	38
PDI[b]	527	80 900	−0.96	−1.22			−3.91	2.30	23
6a	533	66 200	−0.83	−0.98	−1.14	−1.25	−4.04	2.09	23
12a	531	91 600	−0.80	−0.96	−1.07	−1.22	−4.07	2.25	23
18a	684	87 000	−0.46	−0.73	−1.49	−1.66	−4.36	1.76	28
32	608	11 778	−0.59	−0.92	−1.54	−1.78	−4.24	1.86	38

[a] *N*,*N*′-Di(*n*-octyl)naphthalene-1,4,5,8-tetracarboxylic acid diimide. [b] *N*,*N*′-Di(2,6-diisopropylphenyl)perylene-3,4,9,10-tetracarboxylic acid diimide. [c] Estimated by the onset of reduction peaks and calculated according to $E_{LUMO} = -(4.8 + E_{onset})$ eV.

show just a few nanometer red-shifts in the absorption maxima relative to PDI, which may be a reflection of the relatively weak electronic communication of two PDI units.[23,25] Moreover, s-diPDI **6a** possesses broadened absorption traces with a more prominent red-shift of the absorption edge, which can be accounted well for the flexibility of single linkage and different exciton couplings of localized PDI transitions.[23] The hybrid dimer NDI-PDI (**32**) is significantly red-shifted,[38] while the triply linked dimer (**18a**) features the longest absorbance maximum (684 nm), suggesting pronounced red-shifts of about

157 nm regarding to PDI owing to full conjugation through the molecular system.[23,28]

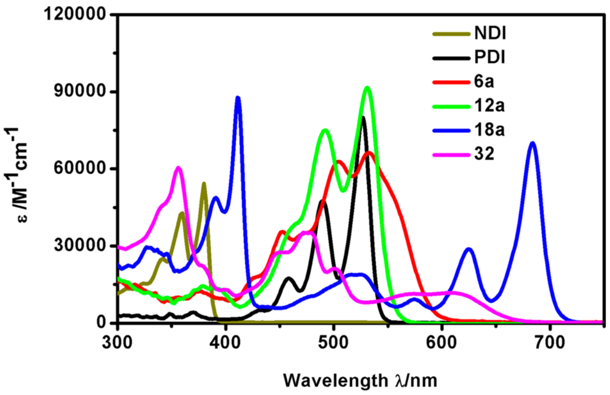

Figure 3. UV−vis absorption spectra of rylene dimers in chloroform: NDI (dark yellow), PDI (black), s-diPDI **6a** (red), d-diPDI **12a** (green), t-diPDI **18a** (blue), and NDI-PDI **32** (magenta).

The first half-wave reduction potentials of these dimers investigated in dichloromethane (vs Fc/Fc$^+$) are more positive than those of NDI and PDI, thereby suggesting the increased electron affinities as a reflection of substantial electronic coupling between the adjacent rylene units. The LUMO levels are −4.04 eV for **6a**, −4.07 eV for **12a**, −4.36 eV for **18a**, and −4.24 eV for **32**, respectively (Table 1). The largely depressed LUMO levels indicate promising as air-stable electron-transporting materials in OFETs and OPVs.

As important representatives, *bay*-linked molecules express totally different equilibrium structures optimized by CAM-B3LYP/6-31G* for their neutral forms, in which it possesses either a flexibly twisted structure with ca. 70° angle between PDI units for singly linked one, or a locked distorted conformation with nearly perpendicularly entangled PDI systems for doubly linked one, or a rigid and almost-planar superstructure in triply linked species.[23] Their structural versatility and designability make them applicable with desired properties in diverse optoelectronic devices.

3.2. Homologous Series of Rylene Arrays

The progressive homologation of *bay*-linked rylene arrays allows us to finely modulate their structures and properties. Examining the singly linked series, from PDI to s-diPDI (**6a**) to s-triPDI (**8**), it is apparent that the single linkage produced much broader absorption spectra and their absorption onsets are gradually red-shifted upon the increase of PDI units.[23] In addition, the introduction of double linkage between the two PDIs does not induce a significant red-shift in solution absorption for both dimer (**14a**) and trimer (**15**), compared with the monomer 1,6,7,12-4ClPDI (**13a**), which is attributed to the limited conjugation by the central twisted eight-membered rings.[25]

In contrast, oligoPDIs with triple linkage revealed a significant bathochromic shift throughout from whole visible to the NIR region, and enhanced electron affinities. By increasing the fused number, the longest absorbance peak reached 684 nm for dimer (**18a**),[23] 750 nm for linear trimer (t-triPDI-2, **29b**), and 805 nm for zigzag trimer (t-triPDI-1, **28b**) (Figure 4). Notably, the UV−vis spectral maxima of their zigzag isomers are definitely bathochromically shifted by about 40−50 nm with respect to those of other isomers, demonstrating a slightly more effective conjugation in zigzag structure. It can be seen that the TDDFT-calculated absorption bands agree well with the observed features in experimental spectra for further assignment of zigzag and linear isomers.[35]

Cyclic voltammograms disclosed that they displayed stronger electron affinity and are capable of accepting two, four, six, and up to eight electrons for PDI, t-diPDI, t-triPDI, and t-tetraPDI, respectively. The changes in reduction values from −0.96 V for PDI, to −0.46 V for t-diPDI, to −0.30 V for t-triPDI-1, to −0.18 V for t-4CltetraPDI-1 have proved remarkable enhancement in the electron-accepting ability by such a bonding way. Thus, the estimated LUMO levels of the series fall from −4.36 eV for dimer to −4.68 eV for tetramer, and more importantly, these values versus the first reduction potentials shows good linear relationship based on monomer PDI (Table 2). As one of the biggest organic conjugated molecules, t-4CltetraPDIs featuring 26 benzene rings and 8 imide groups in structure showed the lowest LUMO level ever reported in the PDI family.[36]

With PDI and NDI as the references, the hybrid arrays NDI-PDI (**32**) and NDI-PDI-NDI (**34a**) possessed absorption maxima bathochromically shifted to about 610 nm,[38] while NDI-diPDI-NDI (**35a**) exhibited absorption maximum at 694 nm.[39] The intensive absorptivity and bathochromic shift are indicative of effective communication and charge delocalization between rylene units. Furthermore, the LUMO levels below −4.2 eV accommodates them for potentially air-stable electron-transporting materials.

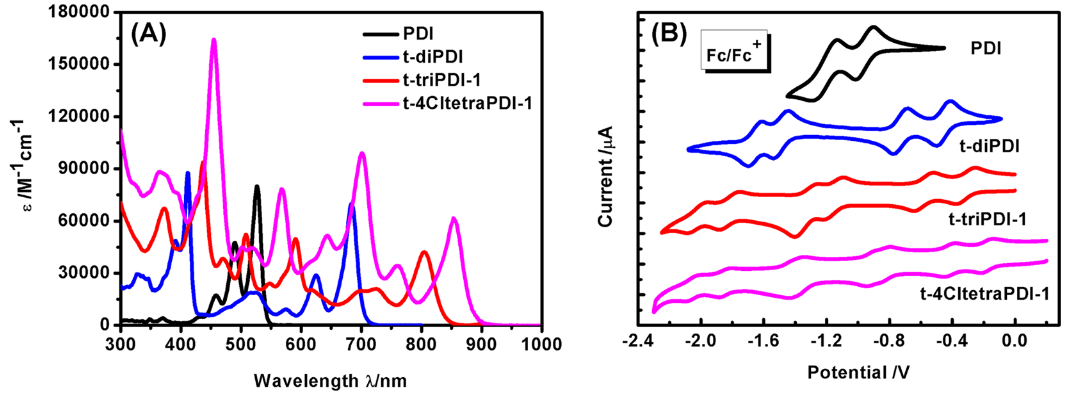

Figure 4. (A) UV−vis absorption spectra in chloroform and (B) reductive cyclic voltammograms in CH_2Cl_2 based on PDI, t-diPDI (**18a**), t-triPDI-1 (**28b**), and t-4CltetraPDI-1 (**30a**).

Table 2. Photophysical Properties of Triply Linked OligoPDIs

compds	λ_{abs} (nm)	E_{1r} (V)	E_{2r} (V)	E_{3r} (V)	E_{4r} (V)	E_{5r} (V)	E_{6r} (V)	E_{7r} (V)	E_{LUMO} (eV)^a	E_g (eV)	ref
t-diPDI (**18a**)	684	−0.46	−0.73	−1.49	−1.66				−4.36	1.76	28
t-triPDI-1 (**28b**)	805	−0.30	−0.57	−1.14	−1.30	−1.80	−1.99		−4.54	1.47	35
t-triPDI-2 (**29b**)	750	−0.33	−0.60	−1.12	−1.26	−1.80	−2.00		−4.51	1.59	35
t-4CltetraPDI-1 (**30a**)	853	−0.18	−0.42	−0.82	−0.92	−1.39	−1.85	−2.05	−4.68	1.39	36
t-4CltetraPDI-2 (**30b**)	813	−0.21	−0.48	−0.84	−0.96	−1.39	−1.85	−2.06	−4.65	1.45	36

^{a}Estimated by the onset of reduction peaks and calculated according to $E_{LUMO} = -(4.8 + E_{onset})$ eV.

3.3. Functionalized Triply-Linked Rylene Dimers

The UV-vis spectra of tetrahalogenated t-diPDIs showed their longest maxima at 656, 661, and 677 nm for t-4CldiPDI (**20a**), t-4BrdiPDI (**22**), and t-4IdiPDI (**23**), respectively, which are hypsochromically shifted relative to t-diPDI (**18a**, λ_{max} = 684 nm), originating from the introduction of the electron-withdrawing halogen atoms on the edges.[29] The single crystal analysis revealed differences in core twisting that the dihedral angle (C14−C15−C16−C17) in t-4CldiPDI was determined to be 34.06°, while it featured a larger torsion angle of 40.25° (C4−C5−C6−C7) in t-4IdiPDI by the reason for larger electrostatic repulsion and steric encumbrance of iodine groups.

Moreover, 2S-diPDI (**25a**, λ_{max} = 633 nm) and 2NPh-diPDI (**25c**, λ_{max} = 670 nm) are significantly blue-shifted from that of **18a**, agreeing well with hypsochromic effect by expanded aromatic core along the short molecular axis. Both of them exhibited extraordinary bowl-shaped structures, and the highest local curvature of PDI bowls in 2S-diPDI was 2.9°, much lower than 4.7° in 2NPh-diPDI, indicating larger strain induced by C−N bonds in pyrrole rings than that by C−S bonds in thiophene rings.[32]

4. LATERALLY EXPANDED RYLENES FOR HIGH PERFORMANCE n-CHANNEL SEMICONDUCTORS

Various applications based on NDI and PDI molecules and corresponding polymers have been achieved.[12] As-investigated laterally expanded rylene dimers are of great important for several fundamental reasons: (i) representing defined molecular topological models of π-electronic structures for both experimental and theoretical researches; (ii) the expanded π-conjugation system for enhancement of molecular stacking and thus favoring electron transport; (iii) depressed LUMO levels by the combination of fused aromatic core and electron-withdrawing imide groups to enhance air stability; (iv) broadened absorbance with high molar extinction coefficients; and (v) tunable molecular self-assembly character by modifying appended chain substituents to improve their solubility and processability. These features allow us to efficiently screen structural series with required properties for employing them in optoelectronic devices.

4.1. Transistor Applications

Among these rylene dyes, those with triple linkage possessing almost planar molecular structures and having low-lying LUMO levels below −4.2 eV, implying promising candidates with impressive n-channel semiconducting characteristics. We first selected a family of triply linked derivatives substituted with different various alkyl chains (t-4CldiPDIs), to examine their performances in solution-processed thin-film transistors. Among them, compound (**20i**) featuring *n*-octadecyl showed a higher mobility of 0.14 cm^2 V^{-1} s^{-1} at the annealing temperature of 160 °C and further demonstrated a maximum mobility up to 0.7 cm^2 V^{-1} s^{-1}.[40] Another molecule **20a** with bulky 2,6-diisopropylphenyl has been proved a mean mobility of 0.03 cm^2 V^{-1} s^{-1} under atmosphere using Langmuir−Schaeffer techniques.[41] In particular, single crystalline micro/nanometer sized ribbons of molecule **20h** were grown via solvent vapor diffusion strategy from toluene/methanol solution (Figure 5). The electron mobility based on these single crystalline transistors fabricated by "Au stripe mask" method exceeded 1.0 cm^2 V^{-1} s^{-1} with the highest value approaching 4.65 cm^2 V^{-1} s^{-1}, one of the highest values reported for air-stable n-channel semiconductors, further demonstrating a bright future of such an n-channel compound in cost-effective organic transistors when combined with device optimization.[42]

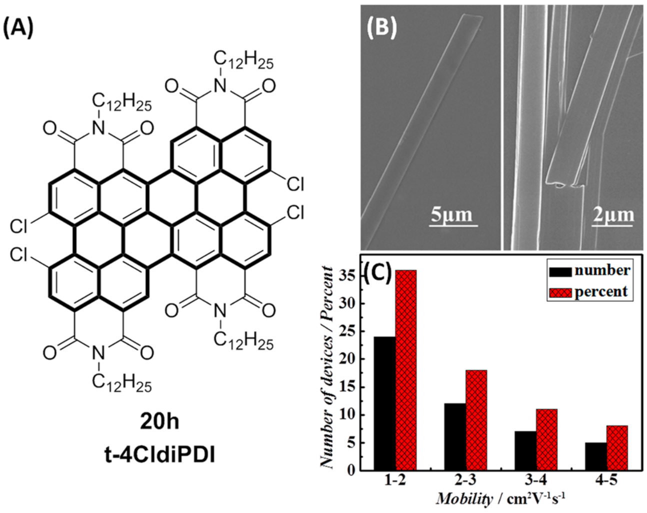

Figure 5. Chemical structures of **20h** (A), SEM image of micro/nanobelts based on **20h** (B), and the distribution of the mobility based on these devices (C).

Further, a preliminary electron mobility of 0.25 cm^2 V^{-1} s^{-1} was obtained for the transistors based on the hybrid structure (**34b**),[38] and remarkable improvement on mobility up to 1.84 cm^2 V^{-1} s^{-1} was achieved through a simple trace-spin-coated technique. While the molecule **35c** with the more expanded structures showed a moderate mobility approaching 0.18 cm^2 V^{-1} s^{-1}.[39]

Very recently, we have elaborated an interesting work of electrical performances based on highly twisted doubly linked diPDIs (**14b−14g**) where the nearly perpendicularly entangled structures are demonstrated to provide an exciting electron mobility reaching 0.16 cm^2 V^{-1} s^{-1} for **14c**. We also examined **24a and 24b** for their electron-transporting properties, and thus a comparable mobility of 0.048 cm^2 V^{-1} s^{-1} based on **24a** film transistors.[26] In view of their resulting chirality, further exploration on transport properties of pure enantiomers or different ratios of mesomers will be a fascinating next project.

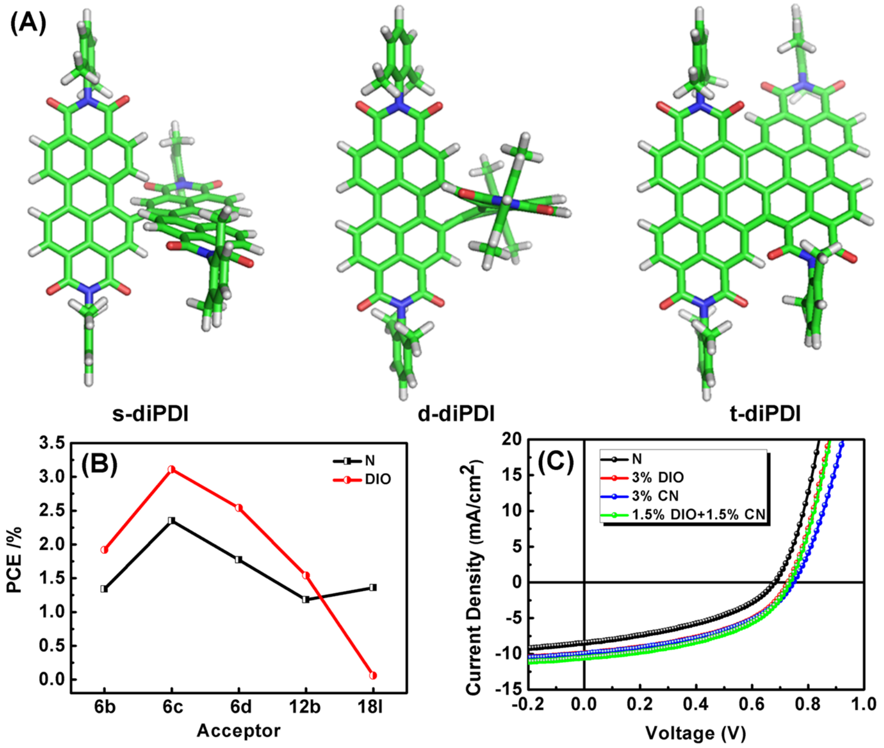

Figure 6. Equilibrium structures (A), comparison of photovoltaic performances of three *bay*-linked diPDIs (B), and *J*−*V* curves based on **6c** (C).

4.2. Photovoltaic Applications

PDI derivatives are promising alternatives serving as non-fullerene electron acceptors in terms of their strong electron affinities, tunable electronic structures and enhanced absorption regarding to fullerene family. Progress has focused on small molecules and polymers based on PDI monomer as electron acceptors to produce moderate PCEs.[43,44] Quite recently, we have demonstrated arrays of solution-processed bulk heterojunction (BHJ) OPVs based on three kinds of *bay*-linked diPDIs decorated by branched alkyl chains (Figure 6). The resulting different degrees of twisting and flexibility in molecular structures combined with introduced branched chains are expected to reduce π-stacked aggregation and modulate crystallinity for ultimately improving the PCEs. Screening three dimers as the acceptor, we found that s-diPDI (**6d**) showed better efficiencies higher than those of d- and t-diPDI analogues (**12b**, **18l**) blending with a 2D conjugated polymer (PBDTTT-C-T). The result agrees well with the design concept that is traceable to tunable crystallinity and interpenetrating nanostructures with favorable charge transport and separation. Thus, alkyl modification on singly linked molecules produced a much better performance of 3.63% for **6c** by the use of the ternary solvent.[24] Further improvement on selecting another 2D conjugated polymer (PBDTBDD) with a down-shifted HOMO level produced a PCE up to 4.39%.[45] By combining molecular, interfacial, and device engineering, the same acceptor demonstrated PCEs close to 6.0%, providing valuable insights on designing novel non-fullerene materials for efficient OPVs.[46]

4.3. Other Applications

Photocharge generation efficiency is crucial for the above photovoltaic devices and other optoelectronic transistors. Based on the triply linked dimer system, the detailed photoconductivity measurement has been carried out by the results of significantly increasing of the internal photocurrent efficiency based on innovative sensitizer t-4CldiPDI **20h** with much higher sensitivity compared to PCBM.[47] Further studies revealed that a dramatic enhancement of photoconductivity by a factor 11 could be observed by incorporating a mixture of polystyrene and the highly conductive *N*,*N*′-diphenyl-*N*,*N*′-bis(3-methylphenyl)-[1,1′-biphenyl]-4,4′-diamine as the charge transporting agent into a photorefractive device.[48] The N-diPDI (**26a**) and PEGylated derivatives are a promising structural platform for the development of effective and photostable photosensitizers for singlet oxygen generation that has found far-reaching applications in a variety of fields.[33]

Accordingly, due to the fast intramolecular electron transfer (ET) progress by the strong driving forces on account of donor−acceptor (D−A) electronic coupling and quite small reorganization energy, the D−A structural N-diPDI systems (**26b** or **26c**) demonstrated their promise as candidates for photosynthesis mimics.[34] Moreover, triply linked systems are being investigated on highly oriented pyrolytic graphite (HOPG) toward controllable assembly and molecular adlayer structures,[49] and the structure-dependent all-optical switching based on these graphene-ribbon-like molecules has also been explored.[50]

5. SUMMARY AND OUTLOOK

Rylene dyes could be harnessed to construct tailor-made molecular arrays with precise lateral expansion. These homologous series of rylenes with a fine-tuned linked nature are particularly exciting and interesting, which provides an impetus to develop fascinating chemistry and reveal informative correlation between molecular structures and electro-optical properties. Their unique features afford a promising library of high performance n-channel organic semiconductors with good ambient stability and processability that meet the required criteria for diverse applications.

AUTHOR INFORMATION

Corresponding Author

*E-mail: wangzhaohui@iccas.ac.cn.

Notes

The authors declare no competing financial interest.

Biographies

Wei Jiang is an Associate Professor in Prof. Zhaohui Wang' group at the Institute of Chemistry, Chinese Academy of Sciences (ICCAS). Her research is presently focusing on the synthesis and functionalization of organic conjugated molecules.

Yan Li is an Assistant Professor in Prof. Zhaohui Wang' group at ICCAS. Her research interests include the design and synthesis of organic functional molecules and their device applications.

Zhaohui Wang is a Professor at ICCAS. He received his B.S. degree (1990) from the Department of Chemical Engineering, Nanjing University of Science and Technology and M.S. degree (1995), Ph.D. degree (1999) from the East China University of Science and Technology. From 1999 to 2005, he stayed in Max-Planck Institute for Polymer Research in Mainz as a research scientist. In 2005, he was appointed as CAS "100 Talents" Scholar and joined the Organic Solids Laboratory, Institute of Chemistry. His research interests include functional conjugated molecules and molecular devices.

ACKNOWLEDGMENTS

The authors are grateful for Professors Daoben Zhu, Lijun Wan, Cornelia Denz, Seth R. Marder, Alex K.-Y. Jen, Fabrizia Negri, Wenping Hu, and Jianhui Hou for fruitful discussions and collaborations. For financial support of this research, we thank the National Natural Science Foundation of China (21225209, 91027043, 91233207, and 21190032), 973 Program (Grants 2011CB932301, 2012CB932903, 2013CB933503 and 2014CB643502), NSFC-DFG Joint Project TRR61, and the Chinese Academy of Sciences (XDB12010000).

REFERENCES

(1) Jiang, W.; Li, Y.; Wang, Z. Heteroarenes as high performance organic semiconductors. *Chem. Soc. Rev.* **2013**, *42*, 6113−6127.

(2) Kim, N.-K.; Khim, D.; Xu, Y.; Lee, S.-H.; Kang, M.; Kim, J.; Facchetti, A.; Noh, Y.-Y.; Kim, D.-Y. Solution-Processed Barium Salts as Charge Injection Layers for High Performance n-Channel Organic Field-Effect Transistors. *ACS Appl. Mater. Interfaces* **2014**, *6*, 9614−9621.

(3) Facchetti, A. Polymer donor-polymer acceptor (all-polymer) solar cells. *Mater. Today* **2013**, *16*, 123−132.

(4) Usta, H.; Newman, C.; Chen, Z.; Facchetti, A. Dithienocoronenediimide-Based Copolymers as Novel Ambipolar Semiconductors for Organic Thin-Film Transistors. *Adv. Mater.* **2012**, *24*, 3678−3684.

(5) Langhals, H.; Knochel, P.; Walter, A.; Zimdars, S. Benzothiadiazoloperylenes and Benzoxadiazoloperylenes: Amorphous Functional Materials. *Synthesis* **2012**, *44*, 3465−3476.

(6) Lin, Y.; Li, Y.; Zhan, X. Small molecule semiconductors for high-efficiency organic photovoltaics. *Chem. Soc. Rev.* **2012**, *41*, 4245−4272.

(7) Lin, Y.; Zhan, X. Non-fullerene acceptors for organic photovoltaics: An emerging horizon. *Mater. Horiz.* **2014**, *1*, 470−488.

(8) Jurchescu, O. D.; Popinciuc, M.; van Wees, B. J.; Palstra, T. T. M. Interface-Controlled, High-Mobility Organic Transistors. *Adv. Mater.* **2007**, *19*, 688−692.

(9) You, J.; Dou, L.; Yoshimura, K.; Kato, T.; Ohya, K.; Moriarty, T.; Emery, K.; Chen, C.-C.; Gao, J.; Li, G.; Yang, Y. A polymer tandem solar cell with 10.6% power conversion efficiency. *Nat. Commun.* **2013**, *4*, 1446.

(10) Zaumseil, J.; Sirringhaus, H. Electron and Ambipolar Transport in Organic Field-Effect Transistors. *Chem. Rev.* **2007**, *107*, 1296−1323.

(11) Clar, E. Oligomers of peri-condensed naphthylens have been termed "rylenes. *Chem. Ber.* **1948**, *81*, 52.

(12) Zhan, X.; Facchetti, A.; Barlow, S.; Marks, T. J.; Ratner, M. A.; Wasielewski, M. R.; Marder, S. R. Rylene and Related Diimides for Organic Electronics. *Adv. Mater.* **2011**, *23*, 268−284.

(13) Würthner, F.; Stolte, M. Naphthalene and perylene diimides for organic transistors. *Chem. Commun.* **2011**, *47*, 5109−5115.

(14) Suraru, S.-L.; Würthner, F. Strategies for the Synthesis of Functional Naphthalene Diimides. *Angew. Chem., Int. Ed.* **2014**, *53*, 7428−7448.

(15) Zhong, Y.; Kumar, B.; Oh, S.; Trinh, M. T.; Wu, Y.; Elbert, K.; Li, P.; Zhu, X.; Xiao, S.; Ng, F.; Steigerwald, M. L.; Nuckolls, C. Helical Ribbons for Molecular Electronics. *J. Am. Chem. Soc.* **2014**, *136*, 8122−8130.

(16) Pschirer, N. G.; Kohl, C.; Nolde, F.; Qu, J.; Müllen, K. Pentarylene- and Hexarylenebis(dicarboximide)s: Near-Infrared-Absorbing Polyaromatic Dyes. *Angew. Chem., Int. Ed.* **2006**, *45*, 1401−1404.

(17) Langhals, H.; Jona, W. Intense Dyes through Chromophore-Chromophore Interactions: Bi- and Trichromophoric Perylene-3,4;9,10-bis(dicarboximide)s. *Angew. Chem., Int. Ed.* **1998**, *37*, 952−955.

(18) Langhals, H. Cyclic carboxylic imide structures as structure elements of high stability. novel developments in perylene dye chemistry. *Heterocycles* **1995**, *40*, 477−500.

(19) Seybold, G.; Wagenblast, G. New perylene and violanthrone dyestuffs for fluorescent collectors. *Dyes Pigm.* **1989**, *11*, 303−317.

(20) Jiang, W.; Li, Y.; Yue, W.; Zhen, Y.; Qu, J.; Wang, Z. One-Pot Facile Synthesis of Pyridyl Annelated Perylene Bisimides. *Org. Lett.* **2010**, *12*, 228−231.

(21) Hassan, J.; Sévignon, M.; Gozzi, C.; Schulz, E.; Lemaire, M. Aryl-Aryl Bond Formation One Century after the Discovery of the Ullmann Reaction. *Chem. Rev.* **2002**, *102*, 1359−1469.

(22) Ma, D.; Cai, Q. Copper/Amino Acid Catalyzed Cross-Coupling of Aryl and Vinyl Halides with Nucleophiles. *Acc. Chem. Res.* **2008**, *41*, 1450−1460.

(23) Jiang, W.; Xiao, C.; Hao, L.; Wang, Z.; Ceymann, H.; Lambert, C.; Di Motta, S.; Negri, F. Localization/Delocalization of Charges in Bay-Linked Perylene Bisimides. *Chem.—Eur. J.* **2012**, *18*, 6764−6775.

(24) Jiang, W.; Ye, L.; Li, X.; Xiao, C.; Tan, F.; Zhao, W.; Hou, J.; Wang, Z. Bay-linked perylene bisimides as promising non-fullerene acceptors for organic solar cells. *Chem. Commun.* **2014**, *50*, 1024−1026.

(25) Zhen, Y.; Yue, W.; Li, Y.; Jiang, W.; Di Motta, S.; Di Donato, E.; Negri, F.; Ye, S.; Wang, Z. Chiral nanoribbons based on doubly-linked oligo-perylene bisimides. *Chem. Commun.* **2010**, *46*, 6078−6080.

(26) Hao, L.; Xiao, C.; Zhang, J.; Jiang, W.; Xu, W.; Wang, Z. Perpendicularly entangled perylene diimides for high performance electron transport materials. *J. Mater. Chem. C* **2013**, *1*, 7812−7818.

(27) Zhen, Y.; Qian, H.; Xiang, J.; Qu, J.; Wang, Z. Highly Regiospecific Synthetic Approach to Monobay-Functionalized Perylene Bisimide and Di(perylene bisimide). *Org. Lett.* **2009**, *11*, 3084−3087.

(28) Qian, H.; Wang, Z.; Yue, W.; Zhu, D. Exceptional Coupling of Tetrachloroperylene Bisimide: Combination of Ullmann Reaction and C-H Transformation. *J. Am. Chem. Soc.* **2007**, *129*, 10664−10665.

(29) Shi, Y.; Qian, H.; Li, Y.; Yue, W.; Wang, Z. Copper-Mediated Domino Process for the Synthesis of Tetraiodinated Di(perylene bisimide). *Org. Lett.* **2008**, *10*, 2337−2340.

(30) Lu, X.; Dong, H.; He, P.; Zhang, X.; Liu, J.; Meng, Q.; Jiang, L.; Wang, Z.; Zhen, Y.; Hu, W. A Ligand-free Copper-promoted Dimerization of Perylene Bisimide by Aromatic C-C Homocoupling and C-H Activation. *Asian J. Org. Chem.* **2013**, *2*, 558−560.

(31) Qian, H.; Liu, C.; Wang, Z.; Zhu, D. S-heterocyclic annelated perylene bisimide: synthesis and co-crystal with pyrene. *Chem. Commun.* **2006**, *46*, 4587−4589.

(32) Qian, H.; Yue, W.; Zhen, Y.; Di Motta, S.; Di Donato, E.; Negri, F.; Qu, J.; Xu, W.; Zhu, D.; Wang, Z. Heterocyclic Annelated Di(perylene bisimide): Constructing Bowl-Shaped Perylene Bisimides by the Combination of Steric Congestion and Ring Strain. *J. Org. Chem.* **2009**, *74*, 6275−6282.

(33) Wu, Y.; Zhen, Y.; Ma, Y.; Zheng, R.; Wang, Z.; Fu, H. Exceptional Intersystem Crossing in Di(perylene bisimide)s: A Structural Platform toward Photosensitizers for Singlet Oxygen Generation. *J. Phys. Chem. Lett.* **2010**, *1*, 2499−2502.

(34) Wu, Y.; Zhen, Y.; Wang, Z.; Fu, H. Donor-Linked Di(perylene bisimide)s: Arrays Exhibiting Fast Electron Transfer for Photosynthesis Minics. *J. Phys. Chem. A* **2013**, *117*, 1712−1720.

(35) Qian, H.; Negri, F.; Wang, C.; Wang, Z. Fully-Conjugated Tri(perylene bisimides): An Approach to the Construction of *n*-Type Graphene Nanoribbons. *J. Am. Chem. Soc.* **2008**, *130*, 17970−17976.

(36) Zhen, Y.; Wang, C.; Wang, Z. Tetrachloro-tetra(perylene bisimides): an approach towards *N*-type graphene nanoribbons. *Chem. Commun.* **2010**, *46*, 1926−1928.

(37) Polander, L. E.; Romanov, A. S.; Barlow, S.; Hwang, D. K.; Kippelen, B.; Timofeeva, T. V.; Marder, S. R. Stannyl Derivatives of Naphthalene Diimides and Their Use in Oligomer Synthesis. *Org. Lett.* **2012**, *14*, 918−921.

(38) Yue, W.; Lv, A.; Gao, J.; Jiang, W.; Hao, L.; Li, C.; Li, Y.; Polander, L. E.; Barlow, S.; Hu, W.; Di Motta, S.; Negri, F.; Marder, S. R.; Wang, Z. Hybrid Rylene Arrays via Combination of Stille Coupling and C-H Transformation as High-Performance Electron Transport Materials. *J. Am. Chem. Soc.* **2012**, *134*, 5770−5773.

(39) Li, X.; Xiao, C.; Jiang, W.; Wang, Z. High-performance electron-transporting hybrid rylenes with low threshold voltage. *J. Mater. Chem. C* **2013**, *1*, 7513−7518.

(40) Zhang, J.; Tan, L.; Jiang, W.; Hu, W.; Wang, Z. *N*-Alkyl substituted di(perylene bisimides) as air-stable electron transport materials for solution-processible thin-film transistors with enhanced performance. *J. Mater. Chem. C* **2013**, *1*, 3200−3206.

(41) Liu, H.; Wu, Y.; Wang, Z.; Fu, H. High performance Langmuir-Schaeffer film transistors based on air stable n-type diperylene bisimide. *Org. Electron.* **2013**, *14*, 2610−2616.

(42) Lv, A.; Puniredd, S. R.; Zhang, J.; Li, Z.; Zhu, H.; Jiang, W.; Dong, H.; He, Y.; Jiang, L.; Li, Y.; Pisula, W.; Meng, Q. High Mobility, Air Stable, Organic Single Crystal Transistors of an n-Type Diperylene Bisimide. *Adv. Mater.* **2012**, *24*, 2626−2630.

(43) Sharenko, A.; Proctor, C. M.; van der Poll, T. S.; Henson, Z. B.; Nguyen, T.-Q.; Bazan, G. C. A High-Performing Solution-Processed Small Molecule: Perylene Diimide Bulk Heterojunction Solar Cell. *Adv. Mater.* **2013**, *25*, 4403−4406.

(44) Zhan, X.; Tan, Z.; Domercq, B.; An, Z.; Zhang, X.; Barlow, S.; Li, Y.; Zhu, D.; Kippelen, B.; Marder, S. R. A High-Mobility Electron-Transport Polymer with Broad Absorption and Its Use in Field-Effect Transistors and All-Polymer Solar Cells. *J. Am. Chem. Soc.* **2007**, *129*, 7246−7247.

(45) Ye, L.; Jiang, W.; Zhao, W.; Zhang, S.; Qian, D.; Wang, Z.; Hou, J. Selecting a Donor Polymer for Realizing Favorable Morphology in Efficient Non-fullerene Acceptor-based Solar Cells. *Small* **2014**, DOI: 10.1002/smll.201401082.

(46) Zang, Y.; Li, C.-Z.; Chueh, C.-C.; Williams, S. T.; Jiang, W.; Wang, Z.; Yu, J.-S.; Jen, A. K.-Y. Integrated Molecular, Interfacial, and Device Engineering towards High-Performance Non-Fullerene Based Organic Solar Cells. *Adv. Mater.* **2014**, *26*, 5708−5714.

(47) Ditte, K.; Jiang, W.; Schemme, T.; Denz, C.; Wang, Z. Innovative Sensitizer DiPBI Outperforms PCBM. *Adv. Mater.* **2012**, *24*, 2104−2108.

(48) Schemme, T.; Travkin, E.; Ditte, K.; Jiang, W.; Wang, Z.; Denz, C. TPD doped polystyrene as charge transporter in DiPBI sensitized photorefractive composites. *Opt. Mater. Express* **2012**, *2*, 856−863.

(49) Wang, H.; Su, H.; Qian, H.; Wang, Z.; Wang, X.; Xia, A. Structure-Dependent All-Optical Switching in Graphene-Nanoribbon-Like Molecules: Fully Conjugated Tri(perylene bisimides). *J. Phys. Chem. A* **2010**, *114*, 9130−9135.

(50) Chen, Q.; Zhang, X.; Chen, T.; Wang, D.; Qian, H.; Wang, Z.; Wan, L. Substitution effect on the adlayer formation of tetrachloroperylene bisimides on HOPG surface. *Surf. Sci.* **2010**, *604*, 2078−2083.